IOPscience iopscience.iop.org

Home Search Collections Journals About Contact us My IOPscience

Temperature dependence of collective excitations in liquid deuterium studied by neutron inelastic scattering

This article has been downloaded from IOPscience. Please scroll down to see the full text article.

1993 J. Phys.: Condens. Matter 5 5743

(http://iopscience.iop.org/0953-8984/5/32/005)

View the table of contents for this issue, or go to the journal homepage for more

Download details:
IP Address: 171.66.16.159
The article was downloaded on 12/05/2010 at 14:18

Please note that terms and conditions apply.

J. Phys.: Condens. Matter 5 (1993) 5743–5754. Printed in the UK

Temperature dependence of collective excitations in liquid deuterium studied by neutron inelastic scattering

F J Mompeán†, F J Bermejo†, M García-Hernández†, B Fåk‡,
J L Martínez§, G Senger¶ and M L Ristig¶

† Instituto de Estructura de la Materia, Consejo Superior de Investigaciones Científicas (CSIC), Serrano 123, E-28006 Madrid, Spain

‡ CEA-CEN Grenoble, 85 X, F-38041 Grenoble Cedex, France

§ Instituto de Ciencias de Materiales, Consejo Superior de Investigaciones Científicas (CSIC), Campus de Cantoblanco, E-28049 Madrid, Spain

¶ Institut für Theoretische Physik, Universität zu Köln, D-5000 Köln 41, Federal Republic of Germany

Received 24 May 1993, in final form 25 June 1993

Abstract. The inelastic response from liquid deuterium has been measured on a thermal three-axis neutron spectrometer at two different temperatures. The observed neutron scattering spectra show clear inelastic features which have been analysed using a damped harmonic oscillator (DHO) model. The momentum transfer dependences of the DHO frequencies and damping coefficients at each temperature are compared and related to the results of the correlated density matrix formalism.

1. Introduction

The liquid hydrogens have played a prominent role in neutron research since the early days and have therefore been extensively studied, especially in connection with, and as a consequence of, the development of cold neutron sources [1]. From the standpoint of the theory of liquids, they constitute an interesting case placed mid-range between liquid ^{3}He and ^{4}He, which are model systems for quantum liquids, and other liquified rare gases and molecular liquids, which for most aspects can be studied within a fully classical formulation. The molecular physics of the free H_2 and D_2 molecules is well described in the literature [2]: the quantum mechanical requirement of the molecular total wavefunction being symmetrical to the interchange of the (composite boson) nuclei presents us with two different (ortho- and para-) rotational and nuclear spin varieties which show very slow interconversion rates; the low mass of the molecules additionally implies large rotational transition energies; the coupling between rotational and nuclear spin states prevents the partition of the scattering cross sections into the standard coherent and incoherent contributions. More recent inelastic neutron scattering studies of H_2 and D_2 have been carried out either at low neutron incident energies [3, 4] or well within the limit of applicability of the impulse approximation [5]. The authors have already reported on the observation of collective excitations in liquid n-D_2 near the triple point using a thermal three-axis neutron spectrometer and have characterized their dispersive properties using a damped harmonic oscillator (DHO) model [6].

The object of the present study is to establish a comparison between the dispersive behaviour at two different temperatures within the liquid range of D_2: near the triple point

0953-8984/93/325743+12$07.50 © 1993 IOP Publishing Ltd

and in the vicinity of the critical point. We have found the use of the damped harmonic oscillator model most convenient since, apart from rendering lineshapes which adequately fit the observed data over a broad range of momentum transfer values, it provides us readily with the basis to obtaining an upper estimate of the DHO frequency by studying the maxima in the spectra of the longitudinal current correlation function derived from the corrected experimental intensities. It is hoped that this study will contribute to ascertain the differences and similarities found in the coherent finite-frequency behaviour of quantum and classical liquids. A further comparison, albeit semiquantitative, will be established between the results of the experimental data analysis and the results of the correlated density matrix theory of quantum fluids [7].

2. Experimental details and data correction

The experimental data reported in this paper have been measured on the DN1 thermal beam three-axis spectrometer at the Siloë reactor of CEN-Grenoble (France). A previous study has been reported on measurements taken at the IN8 spectrometer at the Institute Laue-Langevin High Flux Reactor (Grenoble) [6]. The two instruments are of similar construction and the main significant experimental difference stems from the need of reverting to broader collimations on DN1 as a consequence of the lower neutron flux from the reactor. Also, on IN8 it was possible to fit an evacuated vessel near the sample position to reduce scattering from surrounding air. On both instruments, constant-Q scans using the W configuration were performed at constant incident energy (34.3 meV) selected by using the (002) reflection from a pyrolitic graphite vertically focusing monochromator. On DN1, nominal horizontal collimations of 30, 40, 30 and 30 arc minutes were employed at the in-pile–monochromator, monochromator–sample, sample–analyser and analyser–detector positions, respectively. The energy dependences of the graphite analyser reflectivity and the detector efficiency were neglected throughout the energy and momentum transfer ranges studied. The sample was contained in a cylindrical aluminium can of 1 cm in diameter and 5 cm height in which five cadmium spacers (thickness: 0.03 cm) were inserted in order to reduce multiple scattering to a level $\simeq 5\%$ as estimated using the DISCUS Monte Carlo code [8]. The can was connected to a gas handling rig and inserted into a standard ILL orange-type cryostat. Empty-cell runs for all measured Q-values were taken and a vanadium run was collected by wrapping a vanadium foil around the cell. The sample runs were started by taking a series of constant-Q spectra at a temperature of 20.1 K and under 1 bar of deuterium gas pressure (this thermodynamic state had already been explored on the ILL IN8 instrument). The pressure was subsequently increased to 11 bar, while the temperature of the sample was kept at 20.1 K, and a second set of spectra were taken which does not differ significantly from the low-pressure one as a consequence of the two states having approximately the same density (this dataset will be referred to in this paper with the label 'HP'). Finally, a third set of data was taken at 34.2 K and under 12 bar of deuterium gas pressure (labelled 'HT'). A summary of the liquid thermodynamical parameters [9] and dataset denominations adopted in this paper is given in table 1.

By cooling a room-temperature equilibrium mixture of the ortho- and para-varieties of D_2 (n-D_2) to the experimental temperatures in the absence of catalyser, it is possible to retain the room-temperature relative abundance of both types of molecules (2/3 o-D_2 and 1/3 p-D_2) for times even longer than the duration of the experiment (14 days). This ratio was used throughout the subsequent model calculations.

The following steps were followed in order to obtain, from the experimentally observed intensities, quantities (denoted by $I(Q,\omega)$) representing the convolution of the dynamical

Table 1. Summary of thermodynamical conditions.

Dataset label	T (K)	p (bar)	Density (molecules Å^{-3})
HP	20.1	11	0.0256
HT	34.2	12	0.0188

structure factor of liquid deuterium, $S(Q, \omega)$, with the instrumental resolution, $R(Q, \omega)$:

(i) subtraction of empty-can contribution,

(ii) correction for sample multiple scattering (using the results from the DISCUS Monte Carlo code mentioned above),

(iii) correction to take into account the normalization of the three-axis spectrometer resolution function (i.e. $k_f^3 \cot(\theta_A)$ for a constant k_i scan where θ_A is the Bragg angle at the analyser and k_i and k_f are the neutron incident and final wavevectors).

Figure 1 shows representative spectra at three momentum transfer values for the two temperatures studied in this paper. The feature observed near 12 meV for $Q \geq 0.8$ Å^{-1} can be traced to the empty-can subtraction procedure, due to the fact that empty-cell runs were collected with a more limited energy transfer range. The corresponding data points have been assigned zero weight for the fit. The vanadium run was used to estimate the instrumental resolution function, approximated by a Gaussian profile with full width at half height of 3 meV.

Once the experimental intensities have been corrected, it is possible to analyse them in terms of model dynamical structure factors convolved with appropriate resolution functions or to form a quantity related to the spectrum of the longitudinal current correlation function and denoted by $\bar{J}_L(Q, \omega)$ which can be defined as:

$$\bar{J}_L(Q, \omega) = (\omega^2/Q^2) I(Q, \omega) = (\omega^2/Q^2)(S(Q, \omega) \otimes R(Q, \omega)) \tag{1}$$

where the symbol $\otimes$ denotes a convolution. Figure 2 shows the $\bar{J}_L(Q, \omega)$ experimental currents calculated for those spectra shown in figure 1.

3. Data analysis

The resulting spectra were analysed by fitting a model scattering function convolved with the instrumental resolution function, $R(Q, \omega)$, in energy transfer space. The model has already been described in the literature [6] and is summarized here for the convenience of the reader. The corrected experimental intensities, $I(Q, \omega)$, are related to the proposed scattering model by the following expression:

$$I(Q, \omega) = (S_{self}(Q, \omega) + S_{que}(Q, \omega) + S^I(Q, \omega) + S^M(Q, \omega)) \otimes R(Q, \omega). \tag{2}$$

The precise meanings of the various terms contributing to the model dynamical structure factor are summarized below.

$S_{self}(Q, \omega)$: This term contains the contributions arising from the translational and quantized rotational degrees of freedom, computed for a single isolated molecule. The corresponding formulae can be easily derived from those valid for H_2 and given in the literature [10]. The evaluation of this term has been carried out assuming a room-temperature population ratio for the ortho- and para-varieties. For the liquid phase these expressions are not strictly valid and can be corrected by convolving the gas phase response with a

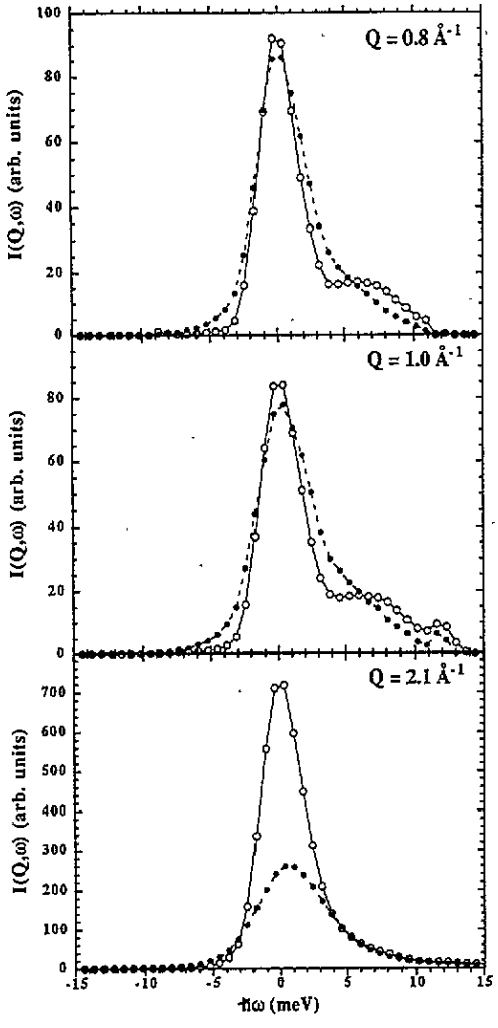

Figure 1. Fully corrected experimental intensities for the three values of the neutron momentum transfer shown and for the two temperatures studied in this paper. Empty circles: 'HP' dataset; Full circles: 'HT' dataset. The definitions of the labels 'HP' and 'HT' are given in table 1. The lines are guides to the eye.

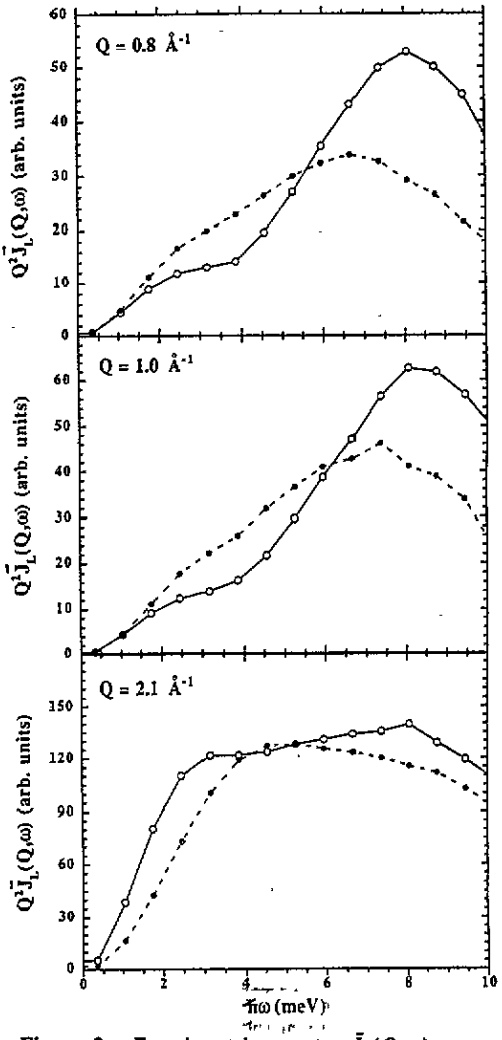

Figure 2. Experimental currents, $\tilde{J}_L(Q,\omega)$, corresponding to the same spectra shown in figure 1. Symbol definitions as in figure 1.

Lorentzian lineshape representing the restricted nature of the diffusive process and adjusting an effective mass parameter in the recoil energy terms.

$S_{que}(Q,\omega)$: This term takes into account the mostly coherent quasielastic response and has been chosen as a Lorentzian lineshape centred at zero-energy transfer with the appropriate detailed balance factor.

$S^I(Q,\omega)$: This term contains the contribution to the response arising from single ('one phonon') collective excitations. The adopted model has been that of a damped harmonic

oscillator (DHO):

$$S^{\mathrm{I}}(Q,\omega) = H(Q)\omega(n(\omega)+1)\frac{4\omega_Q\Gamma_Q}{(\omega^2-\Omega_Q^2)^2+4\omega^2\Gamma_Q^2} \tag{3}$$

formulated in terms of the DHO frequency, Ω_Q, given by:

$$\Omega_Q^2 = \omega_Q^2 + \Gamma_Q^2 \tag{4}$$

where ω_Q is the oscillator 'bare' frequency and Γ_Q is a damping coefficient. $H(Q)$ is an amplitude coefficient and $(n(\omega)+1)$ is the Bose occupation factor. It is noteworthy that at the DHO frequency, the spectrum of the longitudinal current correlation function associated to the response function of the DHO has a maximum, and thus the terms at frequencies close to Ω_Q contribute the most to the second moment of $S^{\mathrm{I}}(Q,\omega)$. This property leads to a straightforward procedure to estimate the upper bound of the DHO frequency by simply inspecting the maxima of the experimental currents, $\bar{J}_{\mathrm{L}}(Q,\omega)$. The use of the DHO model for lineshape fitting has been considered by Fåk and Dorner [11] and Dorner [12] . A rigorous derivation of the above formula is not possible for a disordered system and so we shall just indicate here that usage of the above model in a crystalline medium corresponds to a pseudo-harmonic picture [13].

$S^{\mathrm{M}}(Q,\omega)$: This term represents the multi-excitation contribution to the response. Here a number of approaches, none of them totally satisfactory, are possible. We had adopted initially an estimate cast in terms of a purely incoherent approximation by using the formulae developed for a harmonic crystal [14], evaluated using a density of states rescaled from the solid phase. Subsequently, the multi-excitation contribution was the subject of an extensive parametric study in order to take the double-excitation contribution to the dynamic structure function, $S^{\mathrm{II}}(Q,\omega)$, (analogous to what in a periodic media would be the 'two-phonon' contribution) into account within the coherent approximation, along the lines of the study by Graf *et al* [15] on superfluid ^{4}He. For this purpose, we evaluated numerically the integrals

$$S^{\mathrm{II}}(Q,\omega) = \frac{1}{2(2\pi)^3\rho}\int_0^{q_{\mathrm{cutoff}}}\frac{\hbar Q^2}{2M\Omega_{q_1}}(n(\Omega_{q_1})+1)\frac{\hbar Q^2}{2M\Omega_{q_2}}(n(\Omega_{q_2})+1)$$
$$\times\exp(-CQ^2)\delta(Q-q_1-q_2)\delta(\omega-\Omega_{q_1}-\Omega_{q_2})\mathrm{d}q_1 \tag{5}$$

where ρ is the molecular number density, $\hbar q_1$ and $\hbar q_2$ are the momenta of a pair of excitations, $C \approx 0.5$ Å^2 is an effective mean-square displacement and M denotes the mass of a molecular unit. The Ω_Q values were taken as the DHO frequency estimates from the inspection of the experimental currents, $\bar{J}_{\mathrm{L}}(Q,\omega)$, and the delta function on the frequencies was taken as a Gaussian with a width comparable to the experimental resolution. The main contributions to $S^{\mathrm{II}}(Q,\omega)$ appear as nearly Gaussian lineshapes centred at frequency values corresponding to multiples and combinations of the local maxima and minima in the dispersion relation. The value q_{cutoff} was taken as the higher neutron momentum transfer value at which experimental data were measured. The intensities of the peaks in $S^{\mathrm{II}}(Q,\omega)$ relative to the single-excitation contribution were tabulated as a function of Q and of the thermodynamic state parameters and incorporated to the fitting program by means of narrow Gaussian lineshapes. These contributions, which increase nearly monotonically with Q, do not exceed 20% when $Q = q_{\mathrm{cutoff}}$ for the peaks appearing at the lower energy transfers.

A number of simplifications to the model were introduced in order to reduce the number of fitting parameters and ease the computations. Thus, the single-molecule contribution was not convolved with a diffusive Lorentzian. In practice $S_{\mathrm{self}}(Q,\omega)$ contributes very little to

$I(Q,\omega)$ and the need to revert to using Voigt profiles could be dispensed with. Also, the estimates of the DHO frequencies made from the experimental currents, $\tilde{J}_L(Q,\omega)$, were used as upper bounds for the variation of those fitting parameters.

Some variation in the model parameters, especially in those corresponding to the DHO, is found when the spectra are analysed using the two different proposed schemes for the evaluation of the multi-excitation contribution. These discrepancies are more noticeable and may represent up to 20% of the DHO frequency value for high momentum transfers (specially for momentum transfer values close to the value corresponding to the first maximum of the structure factor, $Q \approx 2$ Å^{-1}) where the multi-excitations are expected to contribute more significantly to the observed response. The multi-excitation contribution was finally restricted to $S^{II}(Q,\omega)$ calculated using equation (5) since no significant improvement in the fitting was found by including the higher-order terms calculated in the incoherent approximation.

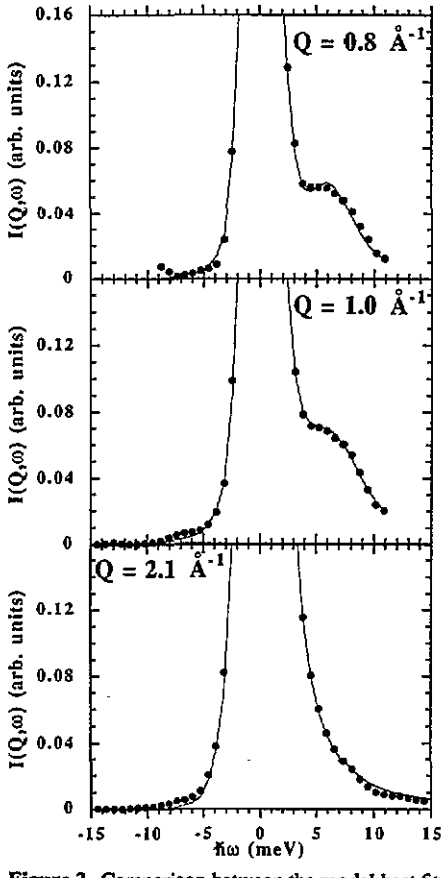

Figure 3. Comparison between the model best fit (solid line) and the experimental data (full circles) for three values of the momentum transfer for the dataset 'HP' taken at 20.1 K and under 11 bar of applied pressure.

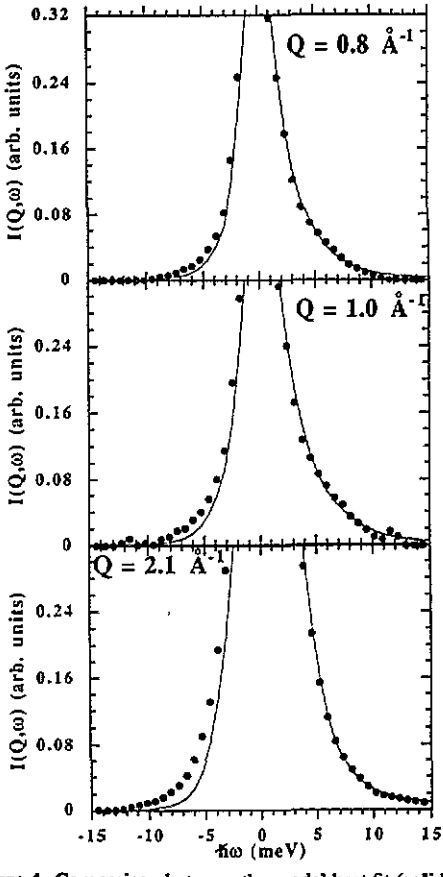

Figure 4. Comparison between the model best fit (solid line) and the experimental data (full circles) for three values of the momentum transfer for the dataset 'HT' taken at 34.2 K and under 12 bar of applied pressure.

4. Results

Figures 3 and 4 show representative fits to the experimental spectra for three values of the momentum transfer at the two temperatures studied in this paper. A good overall agreement was found between the model and the experimental data although certain difficulties have been experienced when trying to fit the tail of the mainly quasielastic response on the neutron energy gain side of the spectra at the higher temperatures. Figures 5, 6 and 7 show the corresponding model contributions to $S(Q,\omega)$. These are depicted before convolving with the experimental resolution. By inspection of these figures it is apparent that the coherent quasielastic and the DHO (single-excitation) contributions dominate the spectra, the latter being especially prominent at non-zero frequencies. The contribution from the $S_{\rm self}(Q,\omega)$ term is barely important and cannot account for the non-zero frequency response due to the observed dispersive behaviour and due to the fact that the zero-frequency contributions from $S_{\rm self}(Q,\omega)$ bear a constant ratio, for a given Q, to the non-zero-frequency ones.

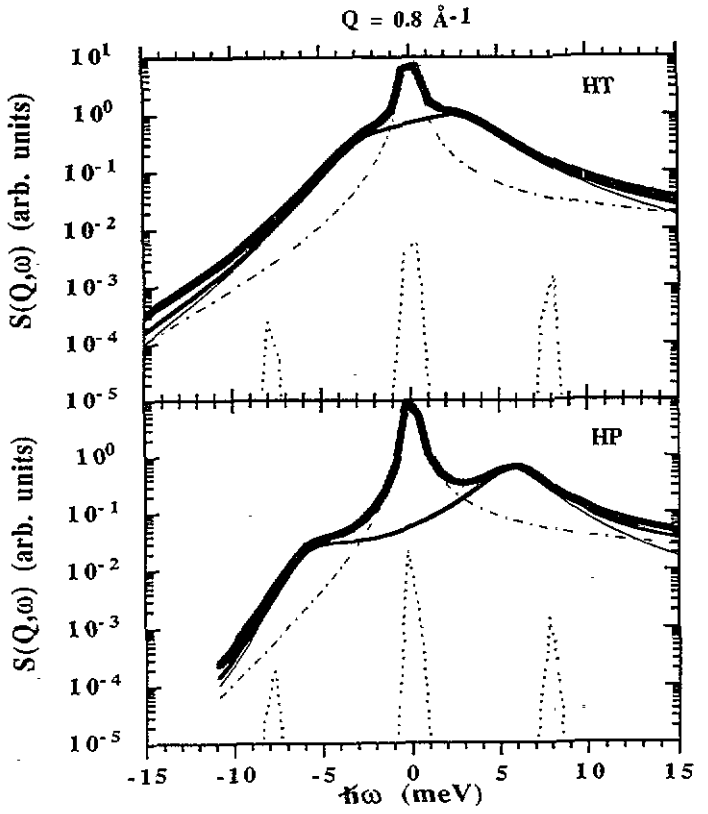

Figure 5. Contributions to the model scattering function, $S(Q,\omega)$, for a momentum transfer $Q = 0.8$ Å^{-1}. The upper and lower frames correspond respectively to the best fits to the 'HT' and 'HP' spectra. The dotted line represents the $S_{\rm self}(Q,\omega)$ contributions. The dashed–dotted line represents $S_{\rm que}(Q,\omega)$. The various continuous lines represent: $S^{\rm I}(Q,\omega)$ (thinner line), $S^{\rm I}(Q,\omega) + S^{\rm II}(Q,\omega)$ (medium thickness) and $S(Q,\omega)$ (wider line).

The momentum transfer dependences of the parameters pertaining to the damped harmonic oscillator contribution to the model are shown in figures 8 and 9. The shape of the curve depicting the dispersive behaviour of the DHO frequency shows, in the three

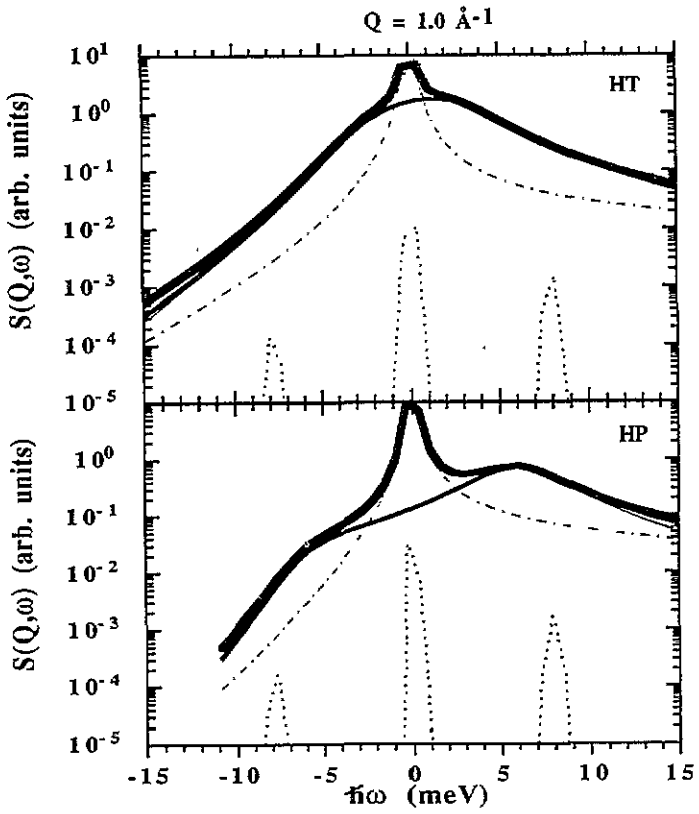

Figure 6. Contributions to the model scattering function, $S(Q, \omega)$, for a momentum transfer $Q = 1.0$ Å^{-1}. The upper and lower frames correspond respectively to the best fits to the 'HT' and 'HP' spectra. Symbol definitions as in figure 5.

cases studied, the regions corresponding to the 'phonon', 'maxon' and 'roton' ranges—if we are to adopt the nomenclature which is in common use for quantum fluids.

The results from the dataset taken at 20.1 K and under 1 bar of pressure are close to those reported from the analysis of the IN8 spectra [6], although as a result of the different approach followed in the estimation of the multi-excitation contributions, the DHO frequencies and damping coefficients are somewhat lower than in our former analysis. Little difference exists between the two thermodynamic states corresponding to 20.1K and 1 and 11 bar regarding the DHO frequency dispersion. Contrary to this fact, the DHO frequencies for the high temperature and pressure point (34.2 K and 12 bar) are consistently smaller for momentum transfers below the maximum in the structure factor ($\simeq 2$ Å^{-1}) and marginally larger for higher momentum transfers. The Q-dependences of the damping coefficients do not differ significatively for the three thermodynamic states. At the lowest measured momentum transfer values, the DHO frequency curves show a positive dispersion behaviour (i.e. they tend to the hydrodynamic limit with excitation energies that are higher than the linear dispersion case evaluated with the measured sound velocities: 1060 and 740 m s^{-1}, respectively, for 20.1 K and 34.2 K under saturated vapour pressure [9]). Their behaviour can be shown to be consistent with that expected for the sound attenuation coefficient, Γ_0,

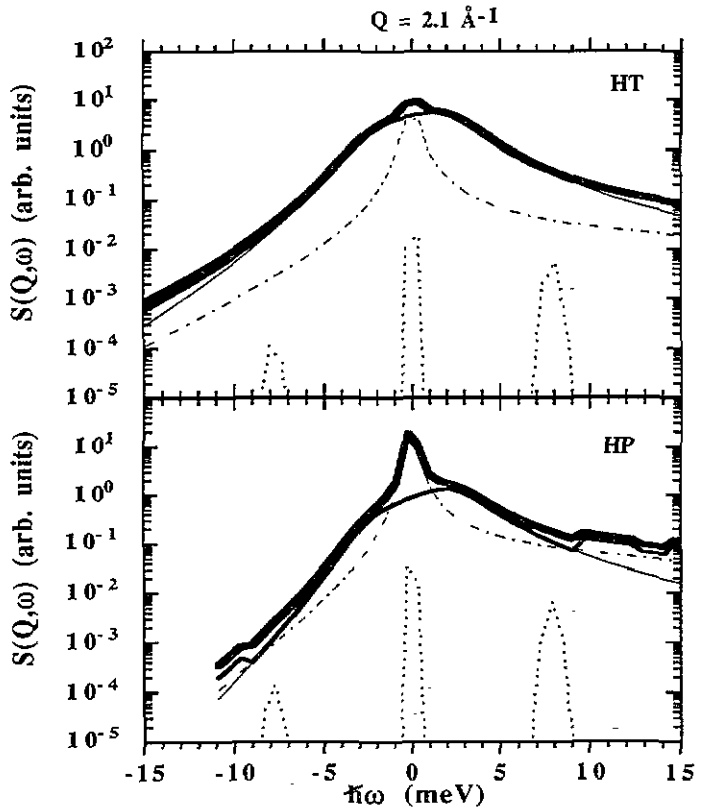

Figure 7. Contributions to the model scattering function, $S(Q,\omega)$, for a momentum transfer $Q = 2.1$ Å^{-1}. The upper and lower frames correspond respectively to the best fits to the 'HT' and 'HP' spectra. Symbol definitions as in figure 5.

in the hydrodynamic limit and neglecting bulk viscosity contributions [16]

$$\Gamma_0 \approx \tfrac{4}{3}\eta_s/\rho + (\gamma - 1)\kappa/c_P\rho \tag{6}$$

since the relative values at the two states of the terms containing the shear viscosity, η_s and thermal conductivity κ yield values for the attenuation of the same order of magnitude (see table 2, data taken from [9]). In equation (6), ρ denotes the density, γ is the adiabatic coefficient and c_P is the heat capacity at constant pressure.

Table 2. Sound attenuation estimates.

	Contributions to sound attenuation (cm^2 s^{-1})		
T (K)	*Shear viscosity*	*Thermal conductivity*	*Total*
20.1	0.0014	0.0003	0.0017
34.2	0.0006	0.0014	0.0020

The temperature- and pressure-dependences of the excitation frequencies can be rationalized in simple terms if one considers that such quantities should, in the classical

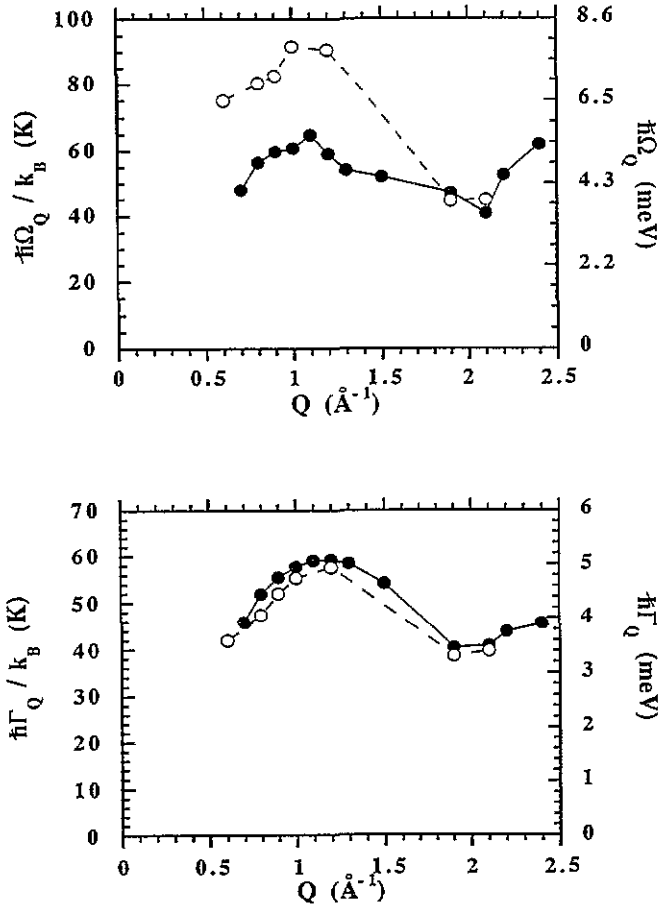

Figure 8. Damped harmonic oscillator frequencies (upper frame) and damping coefficients (lower frame) for the damped harmonic oscillator contributions at the values of the momentum transfer studied. They have been expressed both in temperature and energy units. Open circles: 'HP' dataset; full circles: 'HT' dataset. The straight lines joining the experimental values are guides to the eye.

case, follow a behaviour very much akin to that of the second-frequency moment of a simple monoatomic liquid:

$$\Omega_Q \approx (Q^2 k_B T / M S(Q))^{1/2} \tag{7}$$

where M stands for the total mass of the particle, $S(Q)$ is the static structure factor and the rest of the symbols retain their usual meaning. The main effect of the temperature will be the shift of the position of the roton minimum towards larger values of the momentum transfer since the main peak of $S(Q)$ will move towards larger Q-values due to the decrease in the correlation length. On the other hand, and below Q_p (i.e. the maximum of the structure factor), the value of $S(Q)$ increases with temperature, something which leads to a reduction of the excitation frequencies. It should be noted that, since at low temperatures only small variations in density can be achieved by means of increasing pressure, the most noticeable differences found in this work are caused mainly by temperature effects.

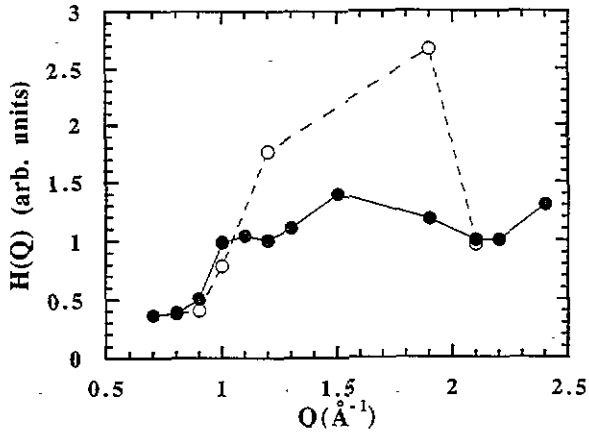

Figure 9. Momentum transfer dependence of the amplitude coefficients, $H(Q)$, for the damped harmonic oscillator contributions. Symbol definitions as in figure 8.

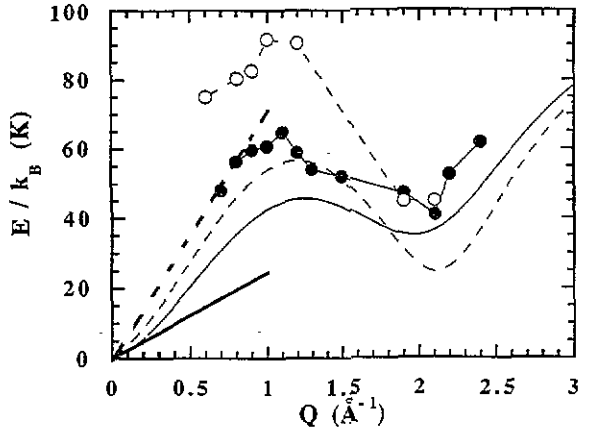

Figure 10. Comparison between the experimental values for the damped harmonic oscillator frequencies and the excitation energies as predicted using the correlated density matrix variational approach. Both magnitudes are expressed in temperature units and plotted as a function of momentum transfer. Experimental values correspond to the 'HP' (open circles) and 'HT' (full circles) datasets. The theoretical prediction is shown for those two thermodynamic states: the dashed curve corresponds to the 'HP' state and the solid curve to the 'HT' state. The two straight lines correspond to the hydrodynamic limit as calculated from the values of the isothermal speed of sound at temperatures of 20 K (dashed straight line) and 34 K (continuous straight line).

5. Comparison with theory

The observed momentum transfer dependences of the DHO frequencies, i.e. the dispersion relations for the characterized excitations, can be compared with the result for the wavevector-dependence of the elementary excitations found in the correlated density matrix formalism [7]. We shall omit here a detailed description of this approach, for which a recent comprehensive summary has appeared in the literature. We shall only briefly mention here that it can be contemplated as a generalization of Feynman's variational *ansatz* for ^{4}He, but that in the present version, the theory neglects any backflow effects. This certainly poses limitations to a quantitative comparison with the model results, where the effects

of damping are important, as has been shown. Figure 10 shows a comparison of the experimental and predicted dispersion relations for the two sets of data at 20.1 K and 11 bar (HP) and 34.2 K and 12 bar (HT). As can be seen, a qualitative agreement exists for the measured momentum transfer range in that the observed temperature behaviour of the DHO frequencies is predicted by the theory. On the other hand, and contrary to what was found for the case of the helium liquids, the presence of a large amount of positive dispersion at all the examined thermodynamic states is also borne out by the theoretical calculation.

6. Conclusions

A model based on a damped harmonic oscillator seems to be an apt description of the observed dispersive coherent inelastic response from liquid deuterium at three different thermodynamic states. Such a model enables us to construct dispersion relations and Q-dependences of damping coefficients showing the qualitative features found in the case of atomic quantum liquids. The effects caused by the pressure and temperature variations are shown to have a clear microscopic correlate in terms of the excitation frequencies and damping factors. A fair amount of positive dispersion is present even at high temperatures. The observations are in qualitative agreement with the results of the correlated density matrix formulation.

Acknowledgments

This work has been supported in part by DGICYT grant No PB89-0037-C03 and by the Deutsche Forschungsgemeinschaft under grant No Ri 267/16-1.

References

[1] Elliot R J and Hartman W M 1967 *Proc. Phys. Soc. (London)* **90** 671
Egelstaff P A, Haywood B C and Webb F J 1967 *Proc. Phys. Soc. (London)* **90** 681
[2] Silvera I F 1980 *Rev. Mod. Phys.* **52** 393
[3] Schott W 1970 *Z. Phys.* **231** 243
[4] Carneiro K, Nielsen M and McTague J P 1973 *Phys. Rev. Lett.* **30** 481
[5] Langel W, Price D L, Simmons R O and Sokol P E 1988 *Phys. Rev.* B **38** 11 275
Herwig K W, Gavilano J L, Schmidt M C and Simmons R O 1990 *Phys. Rev.* B **41** 96
[6] Bermejo F J, Martinez J L, Martin D, Mompean F J, Garcia-Hernandez M and Chahid A 1991 *Phys. Lett.* **158A** 253
Bermejo F J, Mompean F J, Garcia-Hernandez M, Martinez J L, Martin-Marero D, Chahid A, Senger G and Ristig M L 1993 *Phys. Rev.* B **47** 15 097
[7] Senger G, Ristig M L, Kürten K and Campbell C E 1986 *Phys. Rev.* B **33** 7562
[8] Johnson M W 1974 *AERE Harwell Report No 7682*
[9] Roder H M, Childs G E, McCarty R D and Angerhofer P E 1973 *National Bureau of Standards Technical Note No 641, Washington DC*
Guizouarn L 1967 *C.E.A. Serie Bibliographies, No 87, Saclay, France*
[10] Turchin V F 1965 *Slow Neutrons* (Jerusalem: Israel Programme for Scientific Translations)
[11] Fåk B and Dorner B 1992 *Institut Laue-Langevin Report 92FA008S*
[12] Dorner B 1992 *Physica* B **180 & 181** 265
[13] Reissland J A 1973 *The Physics of Phonons* (London: Wiley-Interscience)
[14] Sjölander A 1958 *Ark. Fys.* **14** 315
[15] Graf E H, Minkiewicz V J, Bjerrum-Moeller H and Passell L 1974 *Phys. Rev.* A **10** 1748
[16] Bathia A B 1967 *Ultrasonic Absorption* (Oxford: Clarendon)